

RSC Advances



This is an *Accepted Manuscript*, which has been through the Royal Society of Chemistry peer review process and has been accepted for publication.

Accepted Manuscripts are published online shortly after acceptance, before technical editing, formatting and proof reading. Using this free service, authors can make their results available to the community, in citable form, before we publish the edited article. This *Accepted Manuscript* will be replaced by the edited, formatted and paginated article as soon as this is available.

You can find more information about *Accepted Manuscripts* in the [Information for Authors](#).

Please note that technical editing may introduce minor changes to the text and/or graphics, which may alter content. The journal's standard [Terms & Conditions](#) and the [Ethical guidelines](#) still apply. In no event shall the Royal Society of Chemistry be held responsible for any errors or omissions in this *Accepted Manuscript* or any consequences arising from the use of any information it contains.



Journal Name

COMMUNICATION

Small Molecular Thienoquinoidal Dyes as Electron Donors for Solution Processable Organic Photovoltaic Cells

Received 00th January 20xx,
Accepted 00th January 20xx

Mei-Ju Su,^{a,b} Jin-Hua Huang,^b Li-Peng Zhang,^b Qian-Qian Zhang,^{a,b} Chuan-Lang Zhan,^{b,*} Xue-Qin Zhou,^{a,*} Lian-Ming Yang,^b Yanlin Song,^{b,*} Ke-Jian Jiang^{b,*}

DOI: 10.1039/x0xx00000x

www.rsc.org/

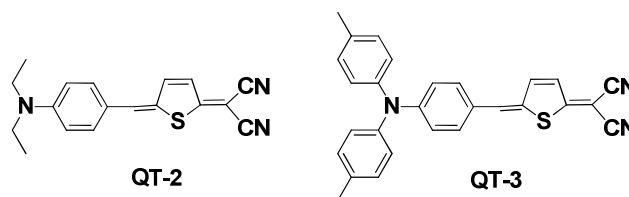
Two small molecular quinoidal thiophene dyes, featuring quinoidal thiophene as spacer, N,N-diethylaniline or N,N-bis(p-methylphenyl)aniline as electron donor moiety, and dicyanomethylene as electron acceptor moiety, have been synthesized as donors for organic photovoltaic cells, and a best power conversion efficiency of 5.12% has been achieved.

During the past two decades, there has been a surge of interest in the development of organic semiconductor materials for organic photovoltaic cells (OPVs), primarily due to their potential low-cost, flexibility and solution processability.¹ In a typical OPV, two components, electron donor and acceptor materials, are combined as active materials in OPVs with a layered or bulk heterojunction structure, where the donor material usually functions as both light harvester and hole transport in the devices. During the past few years, great attention has been focused on the development of low band-gap donor-acceptor (D–A) copolymers, leading to power conversion efficiencies (*PCEs*) of ~10% in a single-junction device.² On the other hand, a large variety of molecular donors, having relatively large molecular weights and complicated structures, were investigated recently, and comparable *PCEs* have been achieved.^{3,4}

Meanwhile, some structurally simple donors with low-molecular-weights, such as squaraines, merocyanines and triphenylamine-based dyes, have attracted great attention for developing simple and low-cost OPVs fabricated using solution

or vacuum deposition technology.^{5,6} These materials can be prepared facilely and readily with scalable synthesis. With merocyanine dyes, Würthner's group achieved a best *PCE* of 4.9% for solution-processed OPVs,^{5c} and 6.1% for vacuum-deposited OPVs,^{5d} measured under standard AM1.5, 100 mW cm⁻² conditions. In the case of triphenylamine-based dyes, a *PCE* of 6.6% was obtained by Wong's group for the devices fabricated by vacuum deposition technology.^{6a}

Quinoidal dyes holds peculiar proaromatic character with high π -conjugated planarity.⁷ Among them, quinoidal oligothiophenes terminated with dicyanomethylenes have been extensively investigated, having n-type or ambipolar behavior with high charge mobilities. Their electronic and optical properties can be adjusted by the extension of the quinoid spacer and the strength of the terminal acceptor and/or donor. In previous reports, push-pull quinoidal dyes were successfully employed as sensitizers in dye-sensitized solar cells.⁸ In this work, two small molecular quinoid dyes, QT-2 and QT-3, shown in Scheme 1, are designed as donor materials for OPVs. In the structures, quinoidal thiophene unit is used as a π -linker terminated with a N,N-bis(p-methylphenyl)aniline or N,N-diethylaniline donor and a dicyanomethylene acceptor at both the ends. With the quinoidal dyes as donor, a best power conversion efficiency of 5.12% has been achieved in organic photovoltaic cells.



Scheme 1 chemical structures of quinoidal dyes QT-2 and QT-3.

The dyes QT-2 and QT-3 can be prepared via simple two step reaction. First, 2-(thiophen-2-yl)malononitrile was synthesized by the Gompper coupling reaction of 2-

RSC Advances Accepted Manuscript

^aSchool of Chemical Engineering and Technology, Tianjin University, Tianjin 300072, China; Collaborative Innovation Center of Chemical Science and Engineering, Tianjin 300072, China.

^bKey Laboratory of Green Printing, Institute of Chemistry, Chinese Academy of Sciences, Beijing, 100190, P. R. China.

E-mail: kjjiang@iccas.ac.cn;

clzhan@iccas.ac.cn

ylsong@iccas.ac.cn

zhouxueqin@tju.edu.cn

Electronic Supplementary Information (ESI) available: Experimental details and additional experimental data. See DOI: 10.1039/c000000x/

iodothiophene with malononitrile according to the method reported previously,⁹ and then followed by Knoevenagel condensation reaction with 4-(diethylamino)benzaldehyde for QT-2 and 4-(di-p-tolylamino)benzaldehyde and QT-3. The synthetic and characteristic details are depicted in Supporting Information. The ¹H and ¹³C spectra are listed in Supporting Information. Both the dyes have good solubility in chlorinated solvents, such as dichloromethane and chlorobenzene, and good film forming ability for solution processed fabrication of BHJ solar cells.

Table 1 Photoelectrochemical properties of QT-2 and QT-3.

| Dye | λ_{max} [nm] | E^a [$M^{-1} cm^{-1}$] | λ_{max}^{opt} [nm] ^a | E_{ox} [V] ^b | HOMO [eV] ^c | LUMO [eV] ^d |
|------|-------------------------|-------------------------------|--------------------------------------------|------------------------------|---------------------------|---------------------------|
| QT-2 | 589 | 1.43×10^5 | 690 | 0.40 | -5.20 | -3.52 |
| QT-3 | 578 | 1.12×10^5 | 714 | 0.55 | -5.35 | -3.55 |

Notes: ^ameasured in CH₂Cl₂ solutions (1×10^{-5} M) at room temperature; ^bOxidation potentials of the dyes were measured in CH₂Cl₂ solutions with tetrabutylammoniumhexafluorophosphate (TBAPF₆, 0.1 M) as electrolyte, Pt wires as working and counter electrode, Ag/Ag⁺ as reference electrode; ^ccalibrated against the Fc⁺/Fc redox couple (4.8 eV below vacuum); ^ddetermined from $E_{LUMO} = E_{HOMO} + E_g^{opt}$.

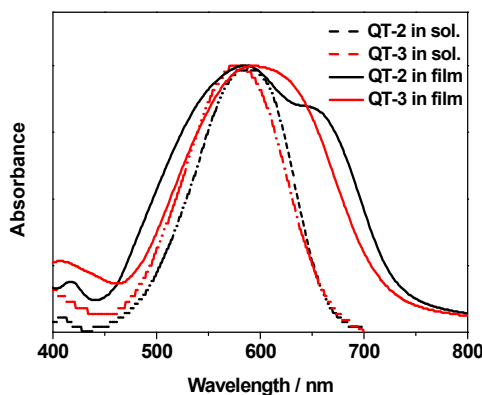


Figure 1 UV-Vis absorption spectra of QT-2 and QT-3 in dilute dichloromethane and thin film.

Figure 1 shows normalized UV-vis absorption spectra of QT-2 and QT-3 in CH₂Cl₂ and solid films, and Table 1 lists the relevant data. In dichloromethane solutions, a strong absorption band was observed in the visible region with maxima at 589 and 578 nm, and extinction coefficients of 1.43×10^5 and 1.12×10^5 M⁻¹ cm⁻¹ for QT-2 and QT-3, respectively. The absorption is much stronger and significantly red shifted in comparison with the dye having a triphenylamine donor and a dicyanovinyl thiophene electron acceptor ($\lambda_{abs} = 501$ nm; $\epsilon = 3.39 \times 10^4$ M⁻¹ cm⁻¹), indicating efficient intramolecular charge transfer in the presence of planar quinoid structure. Compared to the solutions, spin cast thin films of the dyes presented broadening and red-shifted absorption bands extending up to 800 nm due to formation of J-aggregates,

providing favorable light harvesting properties. In case of QT-2, a shoulder at around 660 nm appeared, probably due to crystallization of the molecules.^{5f} Thus, the film absorption of QT-2 is much broader than that of QT-3. The differences can be resulted from more efficient π - π stacking arrangements in QT-2 with high coplanarity in the presence of the planar N,N-diethylaniline donor.

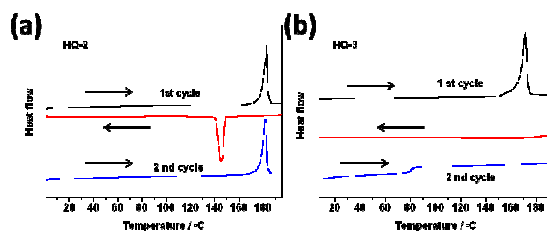


Figure 2 DSC thermogram of QT-2 and QT-3 upon first and second heating and cooling cycles, measured at 10 °C / min under nitrogen.

To study the structural properties, differential scanning calorimetry (DSC) and X-ray diffraction were performed. As shown in Figure 2a, QT-2 exhibited a sharp melting endothermic transition at 182.3 °C on the first heating. After cooling, crystallization was observed at 145.3 °C, and the melting peak appeared again on the second heating. The observations indicate that the QT-2 has a strong tendency to crystallize. In the case of QT-3, melting endothermic transition at 171.5 °C was observed only on the first heating, and no crystallization was observed after cooling. On the second heating, the glass transition at around 80 °C was observed. Moreover, XRD data show that QT-2 has distinct reflection consistent with crystallinity in the neat film as shown in Figure 3a, suggesting ordered aggregation and π - π stacking, which helps improve device performance. The blend, however, show relatively low crystallinity, indicating that the presence of PC₇₁BM acceptor perturbs the packing and texture of QT-2 to some extent. As shown in Figure 3b, amorphous state was observed in both the pristine QT-3 and its blend with PC₇₁BM.

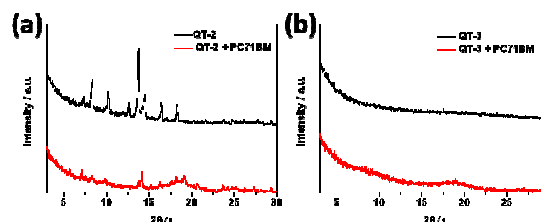


Figure 3 XRD patterns of the films for QT-2 (a) QT-3 (b) and their blends with PC₇₁BM (1:1, w/w), annealed at 90 °C for 10 min.

The electrochemistry properties of QT-2 and QT-3 were measured in dichloromethane solutions by cyclic voltammetry (CV) and differential pulse voltammetry with Fc⁺/Fc as an internal standard. QT-2 and QT-3 exhibited one reversible oxidation wave at 0.40 V and 0.55 V vs Fc/Fc⁺, corresponding to the oxidation of the diethylaniline moiety and the triarylamine, respectively. The energy levels of the HOMO are

-5.20 eV for QT-2 and -5.35 eV for QT-3, determined by cyclic voltammetry calibrated against the Fc^+/Fc redox couple (4.8 eV below vacuum), and the levels of LUMO is -3.52 eV for QT-2 and -3.55 eV for QT-3, determined from $E_{\text{LUMO}} = E_{\text{HOMO}} + E_{\text{g}}^{\text{opt}}$. Both the HOMO and LUMO levels for QT-2 and QT-3 well match with those of PC_{71}BM acceptor (HOMO and LUMO levels are -4.3 eV and -6.1 eV, respectively) with sufficient offsets between the donor and the acceptor.^{4e}

Table 2 Photovoltaic data for QT-2 and QT-3 as donor in OPVs.

| Donor | D-A ratio | J_{sc} mA cm^{-2} | V_{oc} V | FF | PCE (best) % |
|-------|-----------|-------------------------------------|-------------------|------|--------------|
| QT-2 | 2:1 | 6.55 | 0.75 | 0.33 | 1.44 (1.88) |
| | 1:1 | 10.55 | 0.78 | 0.41 | 3.67 (4.02) |
| | 1:2 | 12.94 | 0.80 | 0.43 | 4.56 (5.12) |
| | 1:3 | 11.44 | 0.78 | 0.43 | 4.21 (4.71) |
| QT-3 | 2:1 | 5.26 | 0.74 | 0.29 | 1.08 (1.28) |
| | 1:1 | 7.37 | 0.76 | 0.32 | 1.97 (2.27) |
| | 1:2 | 8.85 | 0.81 | 0.37 | 2.53 (2.98) |
| | 1:3 | 8.51 | 0.81 | 0.34 | 2.37 (2.82) |

Notes: The data are averaged for over 10 devices, with the exception of PCEs, which presents the highest measured values for each condition.

The photovoltaic properties were examined using the dyes as donor in combination with PC_{71}BM as acceptor in typical configuration of ITO/PEDOT:PSS/ PC_{71}BM :QT-2 or QT-3/Ca/Al. Details for the device fabrication are described in Supporting Information. The active layers were deposited from the chlorobenzene solution with different weight ratios of donor/acceptor (D:A = 2:1, 1:1, 1:2, and 1:3), while the thicknesses of the active layers were kept at about 60 nm. The films were annealed at 90°C for 10 minutes before evaporation of the back contact. The open circuit voltage (V_{oc}), short circuit current density (J_{sc}), fill factor (FF), and power conversion efficiency (PCE) under AM 1.5 G simulated solar illumination (100 mW cm^{-2}) are listed in Table 2, the values are averaged from over 10 devices for each condition. At the ratio of 2:1 for QT-2, the device gave a low PCE of 1.88%. With increasing the concentration of the donor in the mixed layer, the J_{sc} s increased dramatically, while the other parameters (V_{oc} and FF) were improved slightly. At the optimized ratio of 1:2, the best device gave a J_{sc} of 13.43 mA cm^{-2} , a V_{oc} of 0.81 V, a FF of 0.47, and a PCE of 5.12%. The corresponding I-V curve and external quantum efficiency (EQE) spectrum of the devices as shown in Figure 4a and 4b, respectively. It can be seen that the device shows broad spectral response across the whole visible region with a maximum value of 65% and about 60% across the range of 500-700 nm, indicative of efficient photoelectron conversion. The integrated J_{sc} (13.32 obtained from the EQE) is well consistent with the value measured by the I-V curve. To the best of our knowledge, the J_{sc} of 13.43 mA cm^{-2} for QT-2 is among the highest values for the solution-processed OSCs with small molecular donors, and QT-2 with molecular weight of 307 is the smallest one among them.^{5,6} In the systems of Table 2, the fill factors (FF) obtained are low, limiting the overall device performance. The similar results were observed in other

solution-processed solar cells with low-molecular weight donors,⁵ and explained due to low charge carrier mobility of the donor dyes as compared with that of the acceptors in the mixed layers.¹⁰ In the case of QT-3, the devices have comparable V_{oc} s but with lower J_{sc} s and FF s compared with those for QT-2 based devices at the same D-A ratio, as shown in Table 2. At the optimized ratio of 1:2, the QT-3-based device gave a J_{sc} of 9.55 mA cm^{-2} , a V_{oc} of 0.82 V, a FF of 0.38, and a PCE of 2.98%.

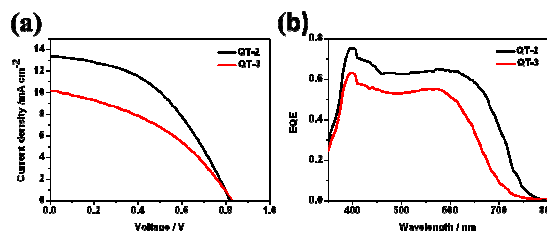


Figure 4 I-V curves (a) and EQE spectra (b) of the optimized devices based on QT-2 and QT-3.

Atomic force microscopy (AFM) was employed to investigate the morphologies of the QT-2 and QT-3 based blend films with PC_{71}BM at the 1:2 ratio. As shown in Figure 5, the AFM topographic images revealed the formation of crystallites, and uniform nanoscale phase separation with bicontinuous networks at the surface for both the films. It is clear that the QT-2 based film show high crystallinity and ordered structures as compared with the QT-3 based film. The root mean square (rms) roughness is 0.35 nm for QT-2 and 0.35 nm for QT-3. To further examine the carrier transportation property, both the electron and hole mobilities were measured with the space-charge-limited current (SCLC) method. The measurements were conducted on the device structure of ITO/TIPD/blend/Al (electron-only) and ITO/PEDOT:PSS/blend/Au (hole-only), respectively. The hole mobilities of the active layers are $3.4 \times 10^{-6} \text{ cm}^2 \text{ V}^{-1} \text{ s}^{-1}$ for QT-2 and $2.1 \times 10^{-6} \text{ cm}^2 \text{ V}^{-1} \text{ s}^{-1}$ for QT-3, with the same electron mobility of $3.0 \times 10^{-3} \text{ cm}^2 \text{ V}^{-1} \text{ s}^{-1}$. The large difference in the mobilities between the donor and acceptor was thought to result in the build-up of space charge,^{5c} partly accounting for the low fill factors obtained.

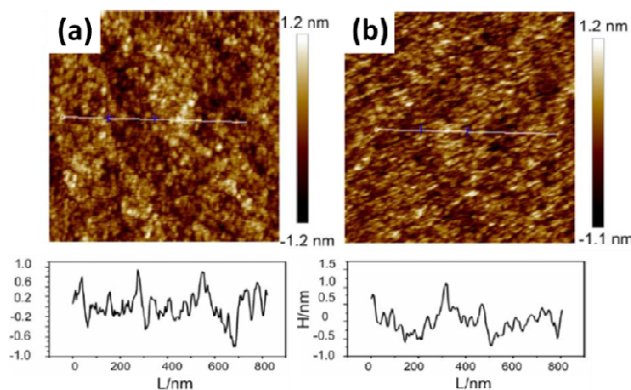


Figure 5 AFM images for the annealed blend films of PC_{71}BM with QT-2 (a) and QT-3 (b).

In summary, two novel quinoidal thiophene dyes, featuring low molecular weight, high molar extinction coefficient, and narrow band-gap, were developed as donors for organic photovoltaic cells. The dyes are structurally simple and can be prepared easily via only two synthetic steps, clearly demonstrating synthetic advantage over current polymeric and molecular donors. The photovoltaic performance was measured in typical BHJ solar cells using the dyes as donor in combination with PCBM acceptor, exhibiting a best power conversion efficiencies of 5.12%. Taking into account the simplicity of the devices, the thin active layers (60 nm), and the low fill factors (~0.47), the result suggests that the quinoidal dyes can be expected to lead to higher performances through optimizing their chemical structures, film morphology, and device architectures.

Acknowledgements

The authors thank the continuous financial support of 973 Program (Nos. 2013CB933004, 2011CB932303 and 2011CB808400), the National Nature Science Foundation (Grant Nos. 61405207, 51473173, 51173190, and 21121001, 21174149, 51373182), and the "Strategic Priority Research Program" of the Chinese Academy of Sciences (Grant No. XDA09020000).

Notes and references

- (a) C. W. Tang, *Appl. Phys. Lett.* 1986, **48**, 183; (b) G. Yu, J. Gao, J. C. Hummelen, F. Wudl, and A. J. Heeger, *Science* 1995, **270**, 1789; (c) F. C. Krebs, *Sol. Energy Mater. Sol. Cells* 2009, **93**, 394; (d) Y. Lin, Y. Li, and X. Zhan, *Chem. Soc. Rev.* 2012, **41**, 4245.
- (a) L. Ye, S. Zhang, L. Huo, M. Zhang, and J. Hou, *Acc. Chem. Res.* 2014, **47**, 1595; (b) J. Chen and Y. Cao, *Acc. Chem. Res.*, 2009, **42**, 1709; (c) Y. He, H.-Y. Chen, J. Hou, and Y. Li, *J. Am. Chem. Soc.* 2010, **132**, 1377; (d) L. Dou, J. You, J. Yang, C.-C. Chen, Y. He, S. Murase, T. Moriarty, K. Emery, G. Li, Y. Yang, *Nat. Photonics* 2012, **6**, 180.
- (a) J. Zhou, Y. Zuo, X. Wan, G. Long, Q. Zhang, W. Ni, Y. Liu, Z. Li, G. He, C. Li, B. Kan, M. Li, and Y. Chen, *J. Am. Chem. Soc.* 2013, **135**, 8484; (b) Y. Liu, C.-C. Chen, Z. Hong, J. Gao, Y. Yang, H. Zhou, L. Dou, and G. Li, *Sci. Rep.*, 2013, **3**, 3356; (c) B. Kan, M. Li, Q. Zhang, F. Liu, X. Wan, Y. Wang, W. Ni, G. Long, X. Yang, H. Feng, Y. Zuo, M. Zhang, F. Huang, Y. Cao, T. P. Russell, and Y. Chen, *J. Am. Chem. Soc.*, 2015, **137**, 3886.
- (a) J. Roncali, P. Leriche, and P. Blanchard, *Adv. Mater.*, 2014, **26**, 3821; (b) B. Walker, C. Kim, and T.-Q. Nguyen, *Chem. Mater.* 2011, **23**, 470; (c) V. Jeux, D. Demeter, P. Leriche, and J. Roncali, *RSC Adv.* 2013, **3**, 5811; (d) Y. Chen, X. Wan, and G. Long, *Acc. Chem. Res.* 2013, **46**, 2645; (e) Y. Sun, G. C. Welch, W. L. Leong, C. J. Takacs, G. C. Bazan, and A. J. Heeger, *Nature Mater.* 2012, **11**, 44.
- (a) F. Silvestri, M. D. Irwin, L. Beverina, A. Facchetti, G. A. Pagani and T. J. Marks, *J. Am. Chem. Soc.*, 2008, **130**, 17640; (b) A. Leliège, C.-H. Le Règent, M. Allain, P. Blanchard and J. Roncali, *Chem. Commun.*, 2012, **48**, 8907; (c) H. Sasabe, T. Igrashi, Y. Sasaki, G. Chen, Z. Hong, and J. Kido, *RSC Adv.* 2014, **4**, 42804; (d) V. Steinmann, N. M. Kronenberg, M. R. Lenze, S. M. Graf, D. Hertel, K. Meerholz, H. Bürckstümmer, E. V. Tulyakova, and F. Würthner, *Adv. Energy Mater.* 2011, **1**, 888; (e) N. M. Kronenberg, V. Steinmann, H. Bürckstümmer, J. Hwang, D. Hertel, F. Würthner, and K. Meerholz, *Adv. Mater.* 2010, **22**, 4193; (f) H. J. Song, E. J. Lee, D. H. Kim, D. K. Moon, S. Lee, *Sol. Energy Mater. Sol. Cells*, 2015, **141**, 232.
- (a) Y.-H. Chen, L.-Y. Lin, C.-W. Lu, F. Lin, Z.-Y. Huang, H.-W. Lin, P.-H. Wang, Y.-H. Liu, K.-T. Wong, J. Wen, D. J. Miller, and S. B. Darling, *J. Am. Chem. Soc.* 2012, **134**, 13616; (b) G. Chen, H. Sasabe, Z. Wang, X.-F. Wang, Z. Hong, Y. Yang, and J. Kido, *Adv. Mater.* 2012, **24**, 2768.
- (a) Y. Suzuki, E. Miyazaki, and K. Takimiya, *J. Am. Chem. Soc.* 2010, **132**, 10453; (b) J. Casado, R. P. Ortiz, and J. T. L. Navarrete, *Chem. Soc. Rev.* 2012, **41**, 5672; (c) Q. Ye, J. Chang, X. Shi, G. Dai, W. Zhang, K.-W. Huang, and C. Chi, *Org. Lett.* 2014, **16**, 3966.
- (a) M. Komatsu, J. Nakazaki, S. Uchida, T. Kubo, and H. Segawa, *Phys. Chem. Chem. Phys.* 2013, **15**, 3227; (b) Q.-Q. Zhang, K.-J. Jiang, J.-H. Huang, C.-W. Zhao, L.-P. Zhang, X.-P. Cui, M.-J. Su, L.-M. Yang, Y.-L. Song, X.-Q. Zhou, *J. Mater. Chem. A*, 2015, **3**, 7695.
- S. Inoue, S. Mikami, K. Takimiya, T. Otsubo, Y. Aso, *Heterocycles*, **2007**, **71**, 253.
- H. Bürckstümmer, N. M. Kronenberg, K. Meerholz, and F. Würthner, *Org. Lett.* 2010, **12**, 3666.

ToC:

Small Molecular Thienoquinoidal Dyes as Electron Donors for Solution Processable Organic Photovoltaic Cells

Mei-Ju Su, Jin-Hua Huang, Li-Peng Zhang, Qian-Qian Zhang, Chuan-Lang Zhan, Xue-Qin Zhou, Lian-Ming Yang, Yanlin Song, Ke-Jian Jiang

Keywords: quinoidal • dye • donor • low molecular weight • organic photovoltaic cell

Two small molecular quinoidal thiophene dyes, featuring low molecular weight, high molar extinction coefficient, and narrow band-gap, have been synthesized as donors for organic photovoltaic cells, and a best power conversion efficiency of 5.12% has been achieved.

